

216-35

121953

P-17

**N93-15043**

**AN EMPIRICAL APPROACH TO PREDICTING LONG TERM BEHAVIOR OF  
METAL PARTICLE BASED RECORDING MEDIA**

By

**Allan S. Hadad  
Ampex Recording Media Corporation  
Redwood City, California**

**Narrative**

**Submitted for the**

**National Space Science Data Center's  
Conference on  
Mass Storage Systems and Technologies for Space and Earth  
Science Applications**

**Goddard Space Flight Center  
Greenbelt, Maryland  
July 23-25, 1991**

12-2-65

**AN EMPIRICAL APPROACH TO PREDICTING LONG TERM BEHAVIOR OF  
METAL PARTICLE BASED RECORDING MEDIA**

Alpha iron particles used for magnetic recording are prepared through a series of dehydration and reduction steps of  $\alpha\text{-Fe}_2\text{O}_3\text{-H}_2\text{O}$  resulting in acicular, polycrystalline, body centered cubic (bcc)  $\alpha\text{-Fe}$  particles that are single magnetic domains. Since fine iron particles are pyrophoric by nature, stabilization processes had to be developed in order for iron particles to be considered as a viable recording medium for long term archival (i.e. 25+ years) information storage. The primary means of establishing stability is through passivation or controlled oxidation of the iron particle's surface.

The usual technique of producing the protective layer is through re-oxidation of the iron particle's surface after synthesis starting with a mixture of 0.1%  $\text{O}_2$  and 99.9%  $\text{N}_2$ . The oxygen content is slowly increased to 20% (the composition of air) so as to maintain the reaction at room temperature. This results in a particle that is stable in air provided it is not subjected to any form of 1) mechanical abuse that could disturb the outer layer, or 2) source of heat that would initiate combustion.

The nature of the passive layer on iron particles has been found to consist of either  $\text{Fe}_3\text{O}_4$ ,  $\gamma\text{-Fe}_2\text{O}_3$  or a mixture of the two. The thickness of the passivation (or total) oxide layer is typically about 3.0 nm. The condition of passivity slows down the oxidation of iron, but, the formation of the iron-oxide layer around metallic iron particles does not preclude further oxidation. The continued stability of iron particles is controlled by the integrity of the oxide layer and the kinetics of diffusion of iron ions through it.

Since iron particles used for magnetic recording are small, additional oxidation has a direct impact on performance especially where archival storage of recorded information for long periods of time is important. Further stabilization chemistry/processes had to be developed to guarantee that iron particles could be considered as a viable long term recording medium.

In an effort to retard the diffusion of iron ions through the oxide layer, other elements such as silicon, aluminum and chromium have been added to the base iron to promote more dense scale formation or to alleviate some of the non-stoichiometric behavior of the oxide or both.

The presence of water vapor has been shown to disrupt the passive layer, subsequently increasing the oxidation rate of the iron.

A study was undertaken to examine the degradation in magnetic properties as a function of both temperature and humidity on silicon-containing iron particles between 50-120°C and 3-89% relative humidity. The methodology to which experimental data was collected and analyzed leading to predictive capability is discussed.

## EXPERIMENT

To study the effect of temperature and humidity on the stability of passivated iron particles as a function of silicon content, three particle batches were prepared from the same precursor containing 0.81, 0.95 and 1.12% silicon by weight.

As stated earlier, the oxidation process of iron particles is diffusion controlled. The increase in oxide thickness is determined by how fast iron ions can migrate to the surface (passivation kinetics). It is assumed that the reduction in  $\sigma_s$  is proportional to the oxide thickness; therefore, Fick's second law of diffusion for concentration dependent systems can be applied:

$$Y^2 \approx D t$$

where:

Y = diffusion distance in cm

D = diffusivity in  $\text{cm}^2/\text{sec}$

t = diffusion time in sec.

For this analysis, the data are plotted as specific magnetic moment versus the square root of time. The resultant slope is therefore the rate of degradation expressed as EMU/gram-sec<sup>0.5</sup> for a given temperature and humidity condition.

Analysis of the interactive effects of temperature, humidity and percent silicon on the degradation of magnetic properties of iron particles were determined using a statistical experimental design package run on an IBM AT compatible computer. The characteristic measured was the log<sub>10</sub> of  $\sigma_s$  loss per second<sup>0.5</sup> (rate of degradation).

The procedure of data analysis consists of selecting an initial mathematical model (usually a quadratic equation to analyze interaction and curvature effects of the form  $Y = C_0 + C_1X_1 + C_2X_2 + C_{13}X_1X_3 \dots + C_{11}X_{12} + C_{22}X_{22} \dots$ ) where  $C_n$  is a constant and  $X_n$  is the level setting of the respective factor. The model is then used to "fit" the data.

## RESULTS AND DISCUSSION

**Dry Conditions.** The first series of oxidation rate experiments were run at the "dry" conditions for the selected temperatures. Oxidation at various temperatures allowed generation of  $\sigma_s$  vs. time curves for iron particles containing 0.81, 0.95 and 1.21% silicon sample at various temperatures.

Figure 1 shows the change in specific magnetic moment with time for the 1.12% silicon sample at various temperatures. As temperature increased, the rate of degradation of  $\sigma_s$  also increased. Differences in the rate of degradation at a given temperature between the three samples studied containing different amounts of silicon are slight, indicating that the iron particles all behave the same at low humidity, independent of Si content or initial  $\sigma_s$  value.

Activation energies for degradation of the 0.81, 0.95 and 1.12% silicon-in-iron powder samples were determined to be 0.383, 0.263, 0.333 eV, respectively when the rates of degradation were plotted against the absolute temperature (Arrhenius plot). Thus, the energy requirement to initiate the oxidation reaction for the various Si-contents is essentially the same and all degrade at essentially the same rate as a function of temperature. However, these activation energies are only ~10% of the value for diffusion of iron through any of the possible iron oxides. The implication is that the primary mechanism for the loss in magnetic properties is not due to lattice diffusion but rather diffusion along some short circuit path such as linear or planer defects present in the oxide shell.

**Moisture Effects.** Magnetic moment loss is shown as a function of humidity at constant temperature (70°C) for the 0.81, 0.95 and 1.12% silicon samples in Figures 2, 3 and 4 respectively. As the humidity increases, the rate at which the magnetic moment degrades increases markedly with decreasing Si content.

Degradation is most rapid for the 0.81% Si-containing iron particles. The sample containing 0.95% silicon is more resistant to degradation until the relative humidity is above 59% at 70°C. Finally, the sample containing 1.12% silicon is the most resistant to degradation exhibiting almost the same rate of loss at 7% relative humidity as it does at 74% relative humidity.

There appears to be a threshold value of relative humidity that is observed at the 0.95% silicon level and possible the 1.12% level, above which the degradation rate increases very rapidly.

As silicon content increases, the critical humidity (the humidity where rapid degradation occurs, at a given temperature) also increases. However, the degradation ceases at  $\sigma_s$  value of 50-60 EMU/gr for the 0.81% silicon sample (Figure 2). The trend appears to be the same (a saturation limit) for the 0.95 and 1.12% Si particles also.

**Interaction of Temperature, Humidity and Silicon.** The three parameters of this study (temperature, percent relative humidity and percent silicon content) interactively influence the degradation of the iron particles. Thus, statistical analysis was performed to quantify the contribution of each variable and present it in a manner that could be easily visualized. The measured characteristic was the  $\log_{10}$  of the degradation rate in specific magnetic moment (EMU/gram-second<sup>0.5</sup>) as derived from the results of the experimental matrix.

The design predictor equation determined using XSTAT is as follows:

$$\begin{aligned} \log_{10} (\text{Rate}) = & -14.76 + 25.26(X_{Si}) + 0.04176(X_{RH}) \\ & + 0.0015(X_T * X_{RH}) - 0.05963(X_{Si} * X_{RH}) \\ & + 0.000068(X_T)^2 - 12.49(X_{Si})^2 \\ & + 0.000219(X_{RH})^2 \end{aligned}$$

where:

$X_{Si}$  = concentration of silicon in weight percent

$X_T$  = temperature in degrees Celsius

$X_{RH}$  = percent relative humidity

The percent variance explained (how well the regression equation predicts the data) was 96.03% so the model can be considered as quite good. Solving the predictor equation via the computer produces two dimensional contour plots of percent relative humidity versus temperature at constant silicon content. The values of constant degradation rate were transferred to a psychrometric chart (Figures 5, 6 and 7) so the relationships between absolute humidity (expressed as pounds of water per pound of dry air), percent relative humidity and temperature as a function of silicon content could be observed. The non-linear degradation behavior becomes very obvious when presented in this manner. A rate value can be taken from the contour plots for a given temperature, humidity and percent silicon content and be used to determine how long it would take for the magnetic moment to degrade to some predetermined value.



For a constant absolute humidity (above the critical value, depending on silicon content) increasing temperature will cause the degradation rate to decrease. It appears that relative humidity is the controlling factor. The corrosion rate appears proportional to the thickness of the adsorbed water layer on the surface of the test specimens. The higher the relative humidity, the thicker the adsorbed layer, hence the faster the corrosion rate.

The behavior observed in the contour plots follows an expression of the form  $\text{Rate} = A_e (b\%RH)_e^{-Q/RT}$ , where at low humidity temperature is the controlling factor, then a transition occurs where humidity effects prevail. It is obvious that special precautions should be taken when attempting to predict long term, low temperature behavior based on high temperature data with a system that is humidity sensitive. Actual archival stability could be less than expected unless humidity control is considered. The value of statistical analysis to the interpretation of oxidation behavior is clearly evident.

### CONCLUSIONS

This study has shown the effects of percent silicon content, temperature and percent relative humidity on pre-passivated fine iron particles used for magnetic recording.

When the iron particles were exposed to various temperatures between 50 and 120°C at very low humidity it was observed that the degradation rates were not affected by either the silicon content or the initial value of the magnetic moment. TEM micrographs revealed that the oxide layer grew thicker leading to a condition of passivity.

It was shown that for a given temperature there exists a critical relative humidity value above which the degradation rate of magnetic moment increases markedly. The presence of silicon appears to increase the critical humidity value at which rapid degradation occurs. When the magnetic moment degrades to 50-60 EMU/gram it remains constant for additional exposure time.

A parametric expression has been proposed to relate silicon content, temperature and humidity to the initial rate of specific magnetic moment degradation for the iron particles used in this study.

Figure 1.

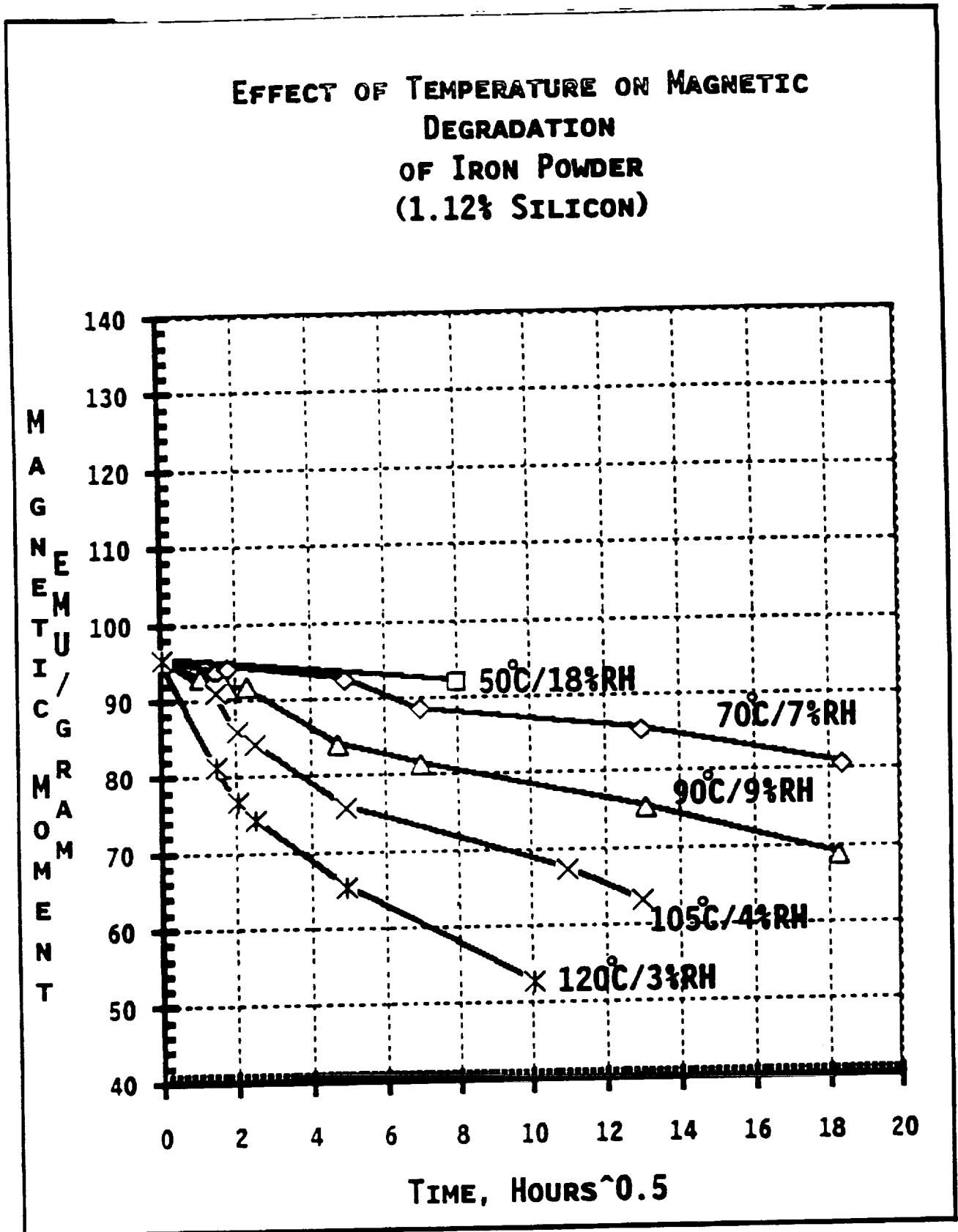


Figure 2.

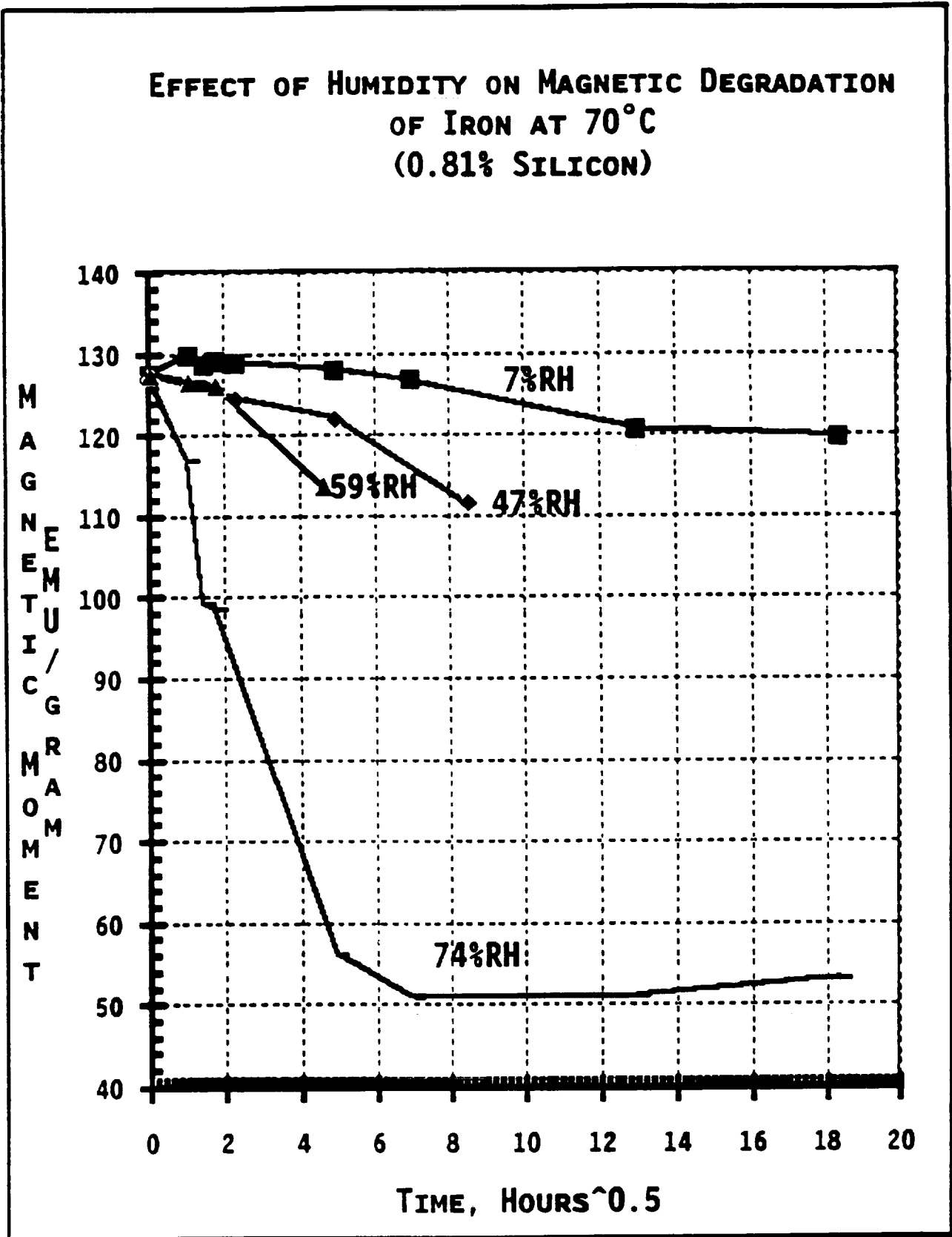


Figure 3.

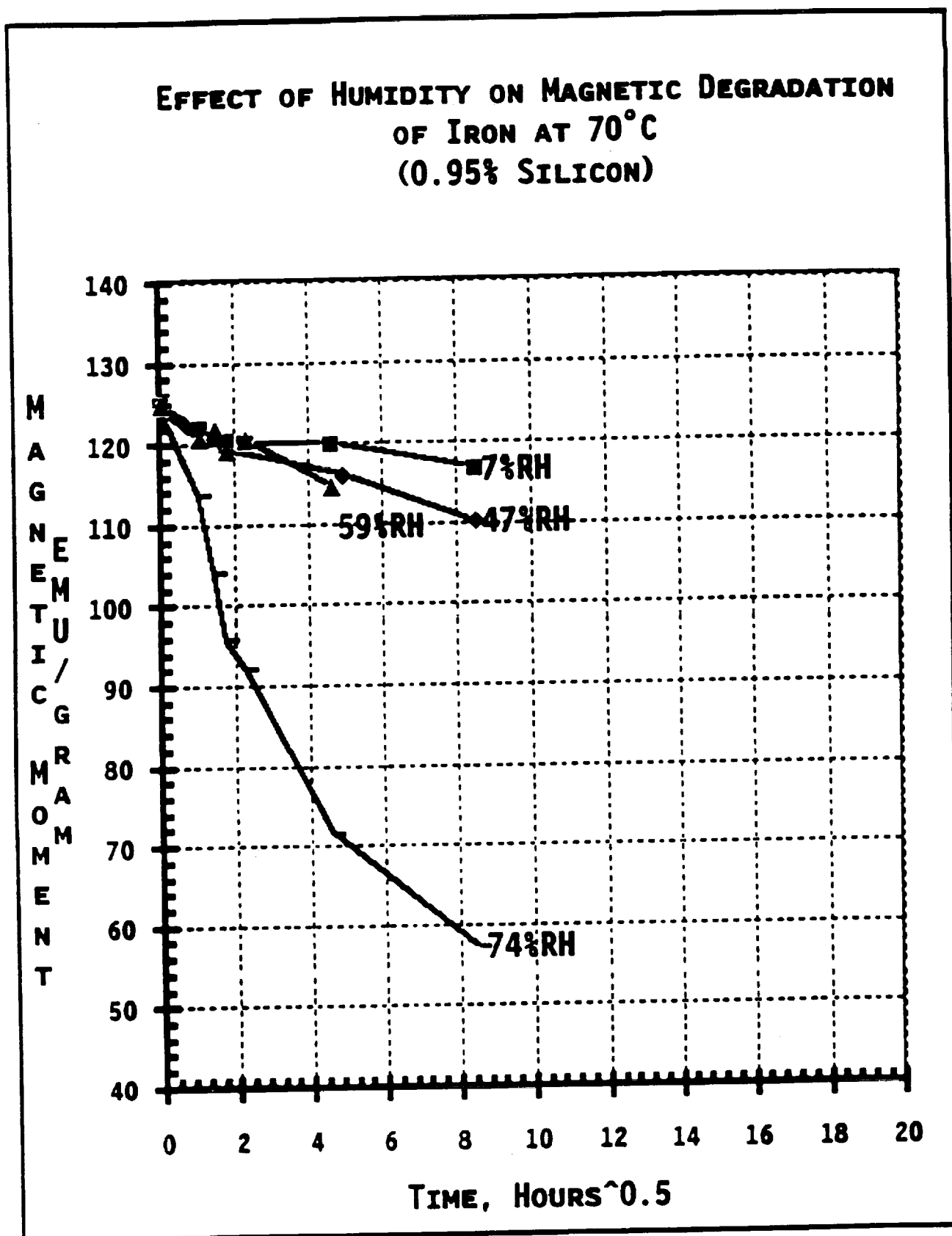


Figure 4.

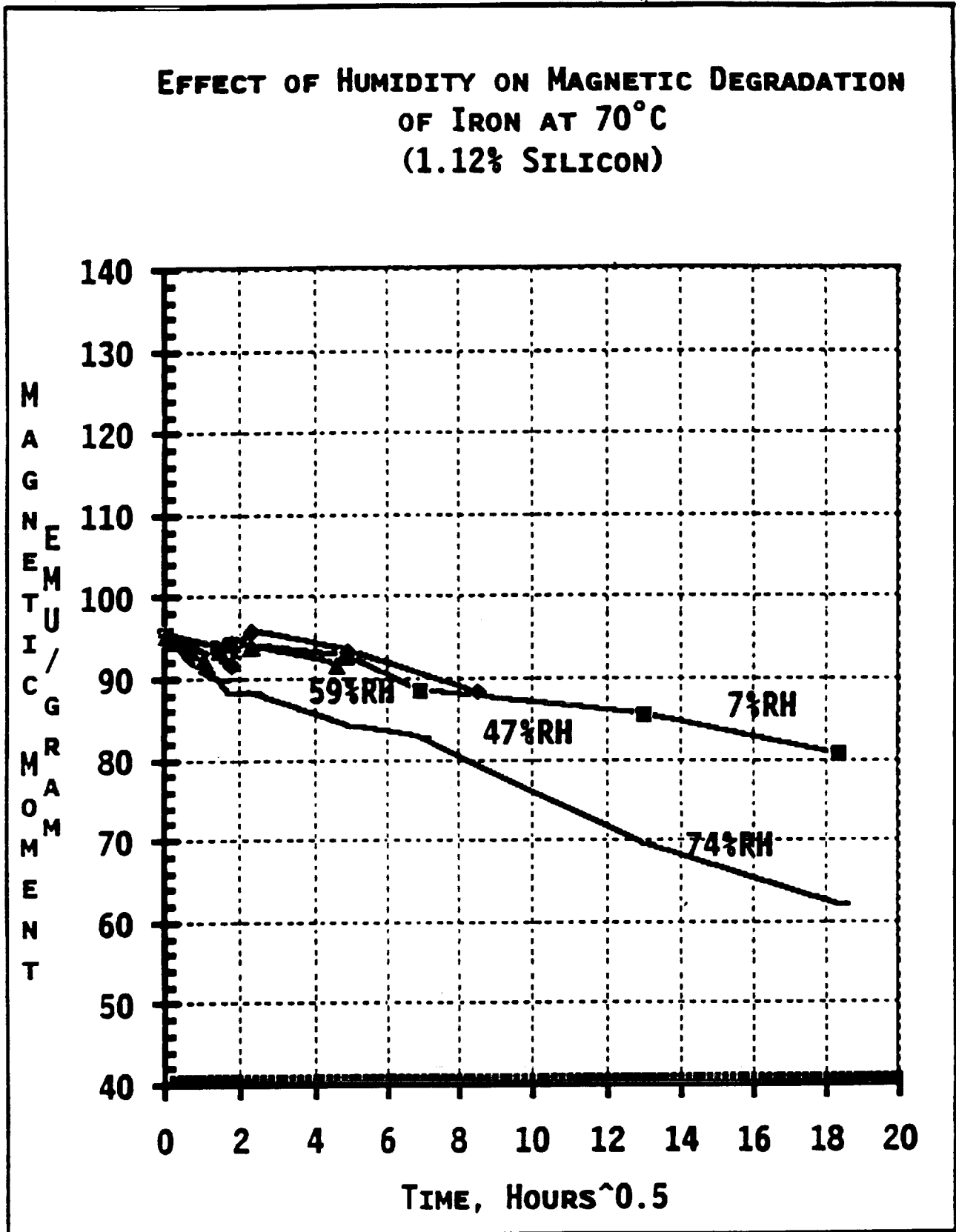


Figure 5.

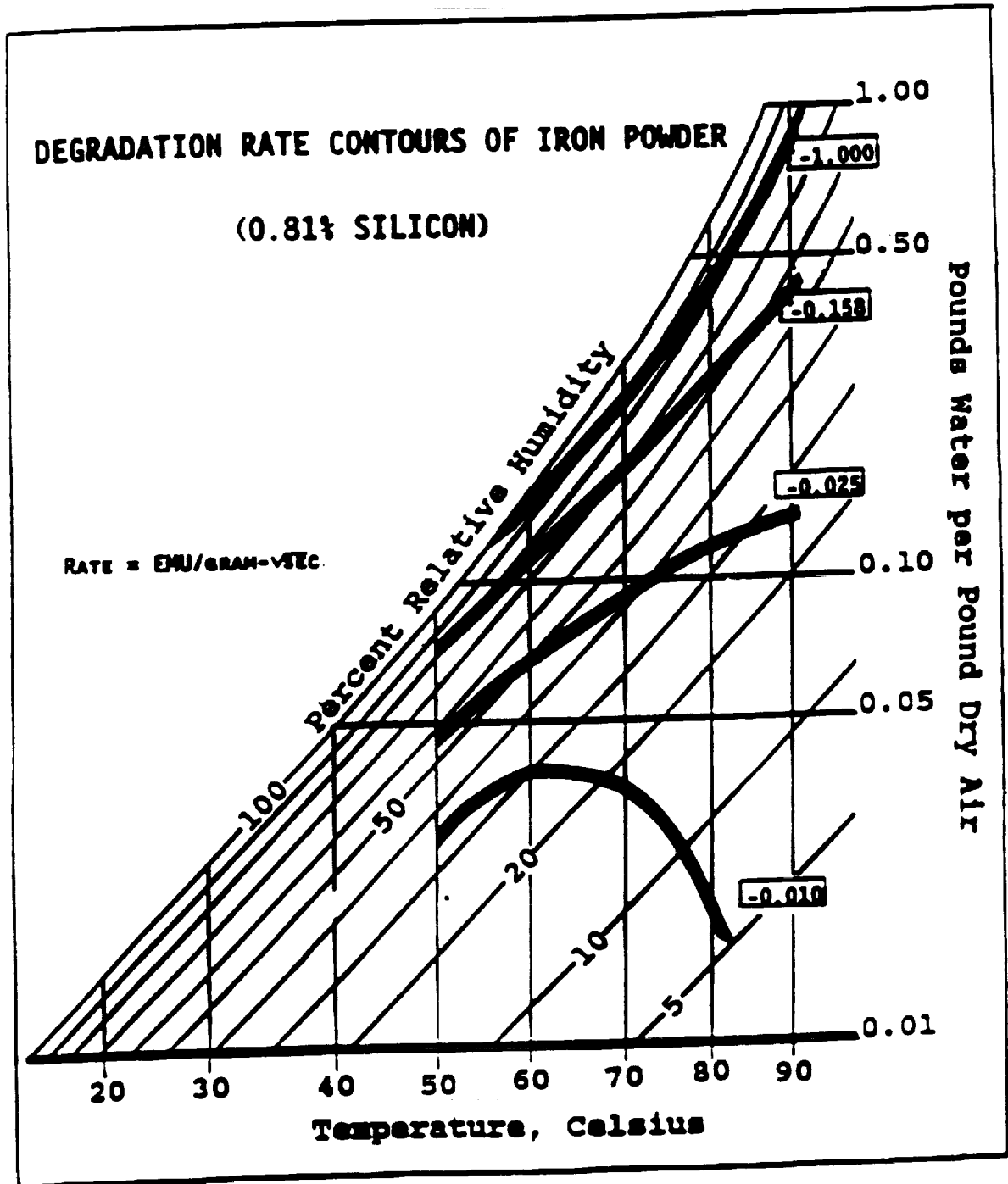


Figure 6.

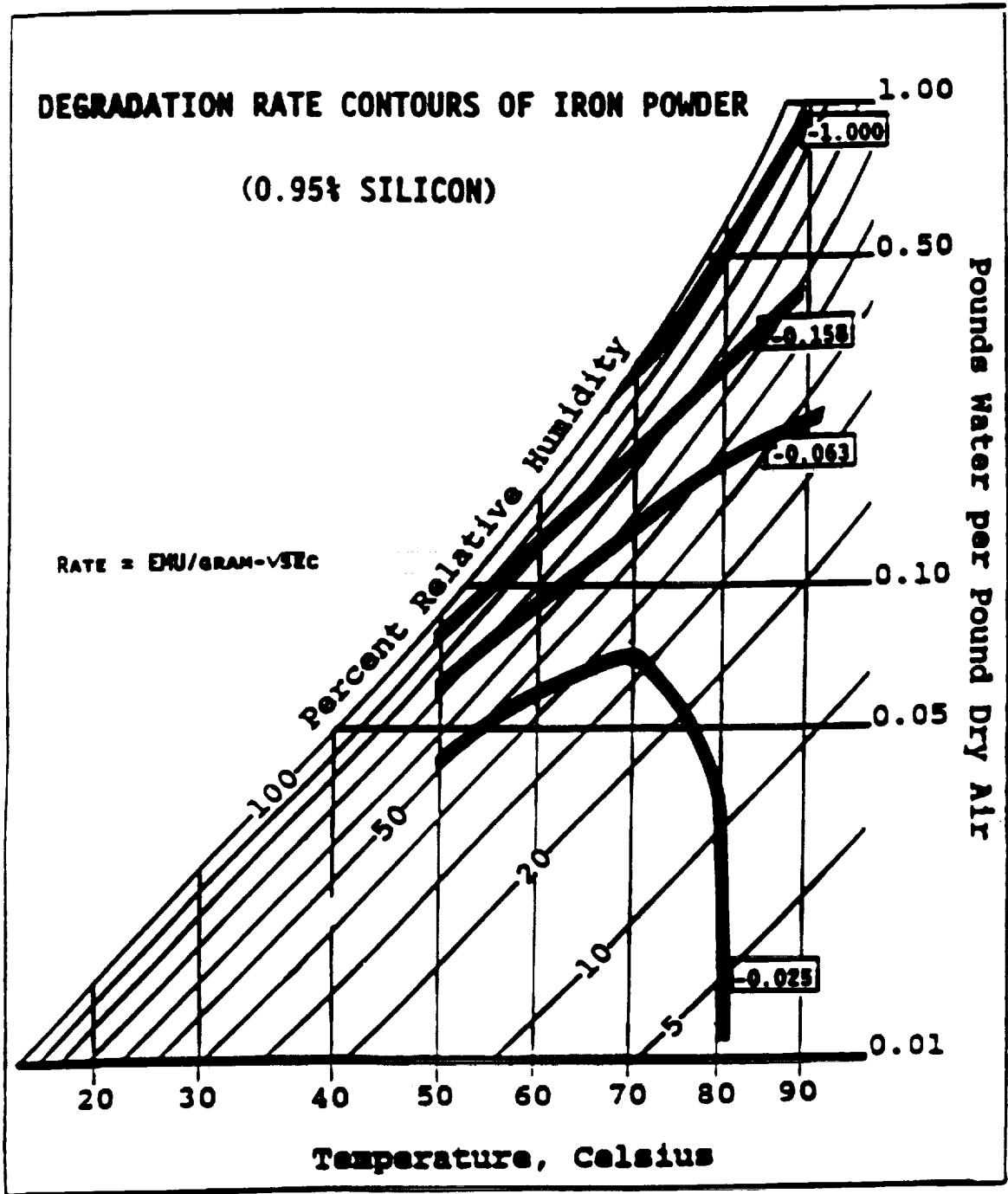




Figure 7.

